

Autotaxin in ascites promotes peritoneal dissemination in pancreatic cancer

Naruomi Jinno  | Michihiro Yoshida  | Kazuki Hayashi  | Itaru Naitoh  |
Yasuki Hori  | Makoto Natsume  | Akihisa Kato  | Kenta Kachi  |
Go Asano  | Naoki Atsuta  | Hidenori Sahashi  | Hiromi Kataoka 

Department of Gastroenterology and Metabolism, Nagoya City University Graduate School of Medical Sciences, Nagoya, Japan

Correspondence

Michihiro Yoshida, Department of Gastroenterology and Metabolism, Nagoya City University Graduate School of Medical Sciences, 1 Kawasumi, Mizuho-cho, Mizuho-ku Nagoya 467-8601, Japan.
Email: mityoshi@med.nagoya-cu.ac.jp

Funding information

Japan Society for the Promotion of Science, Grant/Award Number: KK17K09466

Abstract

Peritoneal dissemination and malignant ascites in pancreatic ductal adenocarcinoma (PDAC) patients represent a major clinical issue. Lysophosphatidic acid (LPA) is a lipid mediator that modulates the progression of various cancers. Based on the increasing evidence showing that LPA is abundant in malignant ascites, we focused on autotaxin (ATX), which is a secreted enzyme that is important for the production of LPA. This study aimed to elucidate the importance of the ATX-LPA axis in malignant ascites in PDAC and to determine whether ATX works as a molecular target for treating peritoneal dissemination. In a PDAC peritoneal dissemination mouse model, the amount of ATX was significantly higher in ascites than in serum. An in vitro study using two PDAC cell lines, AsPC-1 and PANC-1, showed that ATX-LPA signaling promoted cancer cell migration via the activation of the downstream signaling, and this increased cell migration was suppressed by an ATX inhibitor, PF-8380. An in vivo study showed that PF-8380 suppressed peritoneal dissemination and decreased malignant ascites, and these results were validated by the biological analysis as well as the in vitro study. Moreover, there was a positive correlation between the amount of ATX in ascites and the degree of disseminated cancer progression. These findings demonstrated that ATX in ascites works as a promotor of peritoneal dissemination, and the targeting of ATX must represent a useful and novel therapy for peritoneal dissemination of PDAC.

KEYWORDS

autotaxin, malignant ascites, molecular targeted therapy, pancreatic cancer, peritoneal dissemination

Abbreviations: ATX, autotaxin; IVIS, in vivo imaging system; LPA, lysophosphatidic acid; LPARs, LPA receptors; LPC, lysophosphatidylcholine; PBST, PBS Tween 20; PCNA, proliferating cell nuclear antigen; PDAC, pancreatic ductal adenocarcinoma.

This is an open access article under the terms of the Creative Commons Attribution-NonCommercial License, which permits use, distribution and reproduction in any medium, provided the original work is properly cited and is not used for commercial purposes.

© 2020 The Authors. *Cancer Science* published by John Wiley & Sons Australia, Ltd on behalf of Japanese Cancer Association

1 | INTRODUCTION

Pancreatic ductal adenocarcinoma (PDAC) is well-known as one of the cancers with the poorest prognosis, and the 5-year survival rate is reported to be <5%.¹ Compared with gemcitabine, which was the previous standard chemotherapy, new regimens with combined cytotoxic agents, ie, a combination chemotherapy regimen consisting of oxaliplatin, irinotecan, fluorouracil and leucovorin (FOLFIRINOX), and gemcitabine plus nanoparticle albumin-bound paclitaxel (GEM + nabPTX), contribute to a longer survival. However, their efficiency is still far from satisfaction (the median overall survival of metastatic pancreatic cancer is 11.1 months with FOLFIRINOX,² and 8.5 months with GEM + nabPTX³). Even though molecular targeted therapy has an established role in various cancers, it does not achieve the desired therapeutic effects for PDAC.

Lysophosphatidic acid (LPA) is a naturally occurring lipid mediator that acts through G protein-coupled receptors, LPA receptors (LPARs) and modulates a variety of cellular functions; it is present in all mammalian cells and tissues.^{4,5} Through the downstream activation of LPA-LPAR signaling, LPA promotes cell proliferation, invasion, adhesion, angiogenesis, survival, immune evasion, metastasis, and treatment resistance.^{6,7} The regulation of LPA signaling is widely recognized as a promising molecular target for therapy in many fields. Focusing on PDAC, previous studies have reported that LPA signaling plays an important role in the regulation of cellular functions during tumor progression,⁸ and LPA promotes the activities related to cell invasion in PDAC cells,⁹ demonstrating that therapy targeted at LPA signaling is promising.

Among several sources of LPA production, it is widely recognized that LPA in biological fluids is primarily produced by the cleavage of lysophospholipids by the lysophospholipase D enzyme, autotaxin (ATX).^{4,6,10} ATX is an autocrine motility-stimulating factor that was originally identified in the culture supernatant of metastatic melanoma cells.¹¹ Recently, ATX has been reported as a novel target for fibrotic diseases, eg, pulmonary fibrosis¹² and liver fibrosis.¹³ Regarding cancer, previous studies have reported that various cancers secrete higher amounts of ATX, which contributes to cell invasion.¹⁴⁻¹⁷ Interestingly, there is also a report showing that serum ATX activity is increased specifically in PDAC patients.¹⁸

A serious issue of advanced PDAC patients is peritoneal dissemination with malignant ascites, and a significant association between ascites and a poor prognosis has been shown.¹⁹ There is also a report showing that metachronous ascites, which developed during the treatment course, and a massive amount of ascites were poorer prognostic factors.²⁰ The effects of cytotoxic agent therapies provide little therapeutic benefit in such cases,²¹ and the management of the accumulated ascites is challenging.

The components of the LPA signaling pathway are upregulated in a coordinated manner in ascites.²² In fact, the LPA levels in the ascites of ovarian cancer patients are highly elevated.²² It has also been reported that LPA in ascites stimulates the motility of PDAC

cells.²³ This indicated that LPA in ascites must have an important role in the progression of PDAC. However, in terms of the regulation of LPA signaling, no studies have yet proven the existence or elucidated the role of ATX in ascites. To determine a novel therapeutic target for peritoneal dissemination and malignant ascites in PDAC, in this study, we clarified the importance of the ATX-LPA axis and the major role of ATX in ascites. We determined whether the inhibition of ATX activity would attenuate the progression of peritoneal dissemination in a mouse model. We found that inhibition of ATX attenuated LPA signaling via mitogen-activated protein kinase (MAPK) suppression, which resulted in the suppression of PDAC progression in an *in vivo* model as well as in an *in vitro* study. Moreover, our study showed a positive correlation between the tumor volume and the amount of ATX in ascites. We took a particular note of the efficacy of targeting ATX regulation for the treatment of peritoneal dissemination and malignant ascites in PDAC.

2 | MATERIALS AND METHODS

2.1 | Cell cultures

The PDAC cell lines, AsPC-1 (ATCC), PANC-1 (RIKEN Cell Bank), and stably luciferase-transfected AsPC1/luc (JCRB Cell Bank) cells were newly purchased for the present study. Cultures of AsPC-1 and PANC-1 were maintained in RPMI-1640 medium (WAKO Pure Chemical Corporation) supplemented with 10% fetal bovine serum (FBS) in an incubator with 5% CO₂ at 37°C.

2.2 | Wound-healing assay (scratch assay)

A wound-healing assay was conducted to measure cell migration. Cells were grown to confluence in 12-well plates, serum-starved for 24 hours, then a straight wound was made by using a sterile 200- μ L pipette tip. Cells in the plates were followed by the addition of serum-free media with 10 μ mol/L 18:1 lysophosphatidylcholine (LPC; Sigma-Aldrich), 10 μ mol/L 18:1 LPA (Sigma-Aldrich), and 10 μ mol/L ATX inhibitor (PF-8380; Cayman Chemical) at 0 and 24 hours. As the control for LPA, LPC, and PF-8380, the same amount of 0.1% bovine serum albumin (BSA; Sigma-Aldrich) that was used for the dilutions was added into the control wells. The straight wound was photographed and measured under a microscope at 0, 24, and 48 hours. These investigations were carried out in three independent experiments.

2.3 | ATX measurement

Blood and ascites were collected from mice. Using the collected samples, the ATX concentration and activity were measured with an ATX Sandwich ELISA Kit (Echelon Biosciences Inc) and an ATX Activity Kit (Echelon Biosciences Inc), according to the manufacturer's instructions.

2.4 | Animals and model of peritoneal dissemination of PDAC

Female nude mice (BALB/c Slc-nu/nu) aged 7-8 weeks were obtained from Japan SLC. To prepare the *in vivo* peritoneal dissemination model, AsPC1/luc cells were injected intraperitoneally with 1×10^6 cells in 200 μ L of media. All animal experiments were performed using protocols approved by the Institutional Animal Care and Use Committee of Nagoya City University Graduate School of Medical Sciences.

2.5 | *In vivo* experiments and bioluminescence imaging

One day after the implantation, the mice were randomly allocated into two groups. The ATX inhibitor, PF-8380, was solubilized in 2:1 dimethyl sulfoxide (DMSO, WAKO Pure Chemical Corporation)-saline and injected intraperitoneally at the dose of 10 mg/kg twice a day for 3 weeks. Control animals received DMSO-saline as the control. Every week after the implantation of cells, bioluminescence was measured using a multifunctional *in vivo* imaging system (IVIS; MIIS, Molecular Devices Japan) to monitor the disseminated cells. For scanning by IVIS, the mice were anesthetized and intraperitoneally injected with D-luciferin (150 μ g/g; WAKO Pure Chemical Corporation) diluted in PBS. We acquired monochrome photographs and *in vivo* fluorescence images by bioluminescence acquisition for 3 minutes. Mice without any fluorescence signal detected under IVIS at 1 week after the implantation were excluded from this study. The total luminescence flux on Days 9, 16, and 23 was quantified using MetaMorph-MIIS software (Molecular Devices Japan) to calculate the total volume of disseminated tumor. The body weight of the mice was monitored twice a week. On day 23, the mice were sacrificed. The peritoneal disseminated tumor samples, serum, and ascites were collected for biological analysis.

2.6 | Statistical analysis

The statistical significance of differences was determined using Student's *t* test as appropriate. Regression analysis was performed with the data obtained from the *in vivo* study. Differences were considered statistically significant at $P < .05$. Data are expressed as the mean \pm standard error (SE).

We described fundamental materials and methods in Appendix S1.

3 | RESULTS

3.1 | A significant amount of ATX was present in malignant ascites

Based on the evidence that peritoneal dissemination with ascites is found at high frequency in advanced PDAC patients, and that the presence of ascites is recognized as a poor prognostic factor, we first

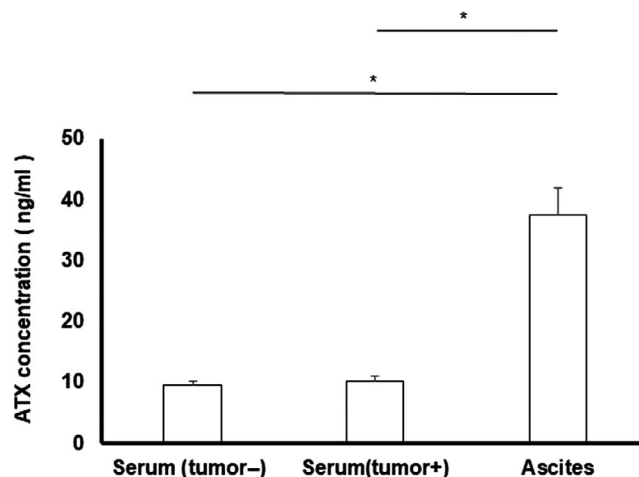


FIGURE 1 Autotaxin (ATX) concentration in nude mice and the peritoneal dissemination model of pancreatic ductal adenocarcinoma (PDAC). Measurement of ATX concentration in nude mice and the peritoneal dissemination model. We checked ATX concentration in the sera of mice with or without tumors and in ascites in the peritoneal dissemination model. The mean of ATX concentration in sera obtained from mice without tumors ($n = 7$) and in the sera and ascites from mice with tumors on day 23 after AsPC1/luc cell implantation ($n = 8$). Bars, standard error; * $P < .001$

investigated the presence of ATX in ascites with the murine peritoneal dissemination model. Sera from mice with intraperitoneally implanted tumors did not show a significant increase in ATX ($n = 8$; 10.4 ± 0.7 ng/mL) compared with the sera of the control mice ($n = 7$; 9.6 ± 0.6 ng/mL). However, ascites in mice with intraperitoneally implanted tumors had significantly higher amounts of ATX ($n = 8$; 37.6 ± 4.5 ng/mL) than the sera ($P < .001$; Figure 1). In addition, we confirmed that ATX activity showed similar findings to ATX concentration (Figure S1). These results indicated that ascites have a significantly increased amount of ATX in peritoneal dissemination of PDAC.

3.2 | LPA promoted the migration, proliferation, and phosphorylation of ERK1/2 and AKT in PDAC cells

To evaluate the effects of LPA on PDAC cell migration, we conducted the wound-healing assay. AsPC-1 and PANC-1 were confirmed to have the significant expression of ATX (Figure S2), so we selected AsPC-1 and PANC-1 in this study. As expected, LPA significantly promoted cell migration in both AsPC-1 (48 hours, $23\% \pm 3.1\%$ vs $41\% \pm 1.7\%$, $P < .01$) and PANC-1 (48 hours, $29\% \pm 2.9\%$ vs $60\% \pm 1.1\%$, $P < .001$) cells (Figure 2A-D). We also confirmed that cell proliferation was significantly promoted in AsPC-1 (cell number; 48 hours, $12.9 \times 10^4 \pm 0.7 \times 10^4$ vs $15.6 \times 10^4 \pm 0.2 \times 10^4$, $P < .01$) and PANC-1 (48 hours, $23.2 \times 10^4 \pm 1.5 \times 10^4$ vs $31.5 \times 10^4 \pm 0.6 \times 10^4$, $P < .01$) cells (Figure S3A,B).

The MAPK pathway and phosphatidylinositol-3-kinase (PI3K) pathway is well-known as the major downstream pathways of LPA-LPAR signaling. To confirm the biological status of the signaling activated by LPA, the phosphorylation of ERK1/2 and AKT was examined in AsPC-1

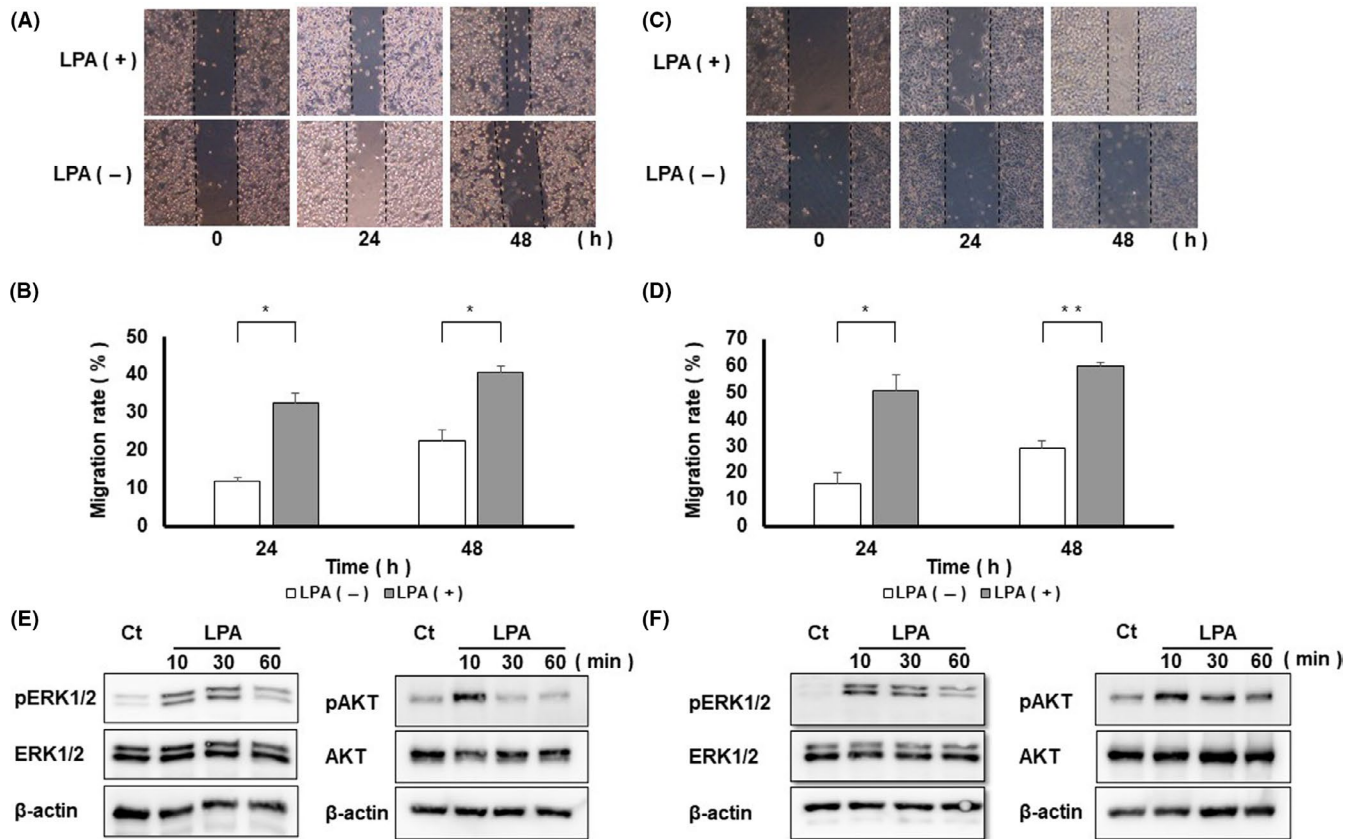


FIGURE 2 Cell migration and protein expression in AsPC-1 and PANC-1 cells. Representative images obtained at 0, 24, and 48 h after a scratch wound was made in confluent monolayers of AsPC-1 (A) and PANC-1 (C) cells. At 0 and 24 h after the scratch, 10 $\mu\text{mol/L}$ lysophosphatidic acid (LPA [+]) or 0.1% BSA (LPA [-]) was added. Quantification of the wound-healing assay in AsPC-1 (B) and PANC-1 (D) cells. Data represent the means of three independent experiments. Bars, standard error; * $P < .01$; ** $P < .001$. Western blotting analysis of ERK1/2 and AKT phosphorylation after the addition of 10 $\mu\text{mol/L}$ LPA in AsPC-1 (E) and PANC-1 (F) cells

and PANC-1 cells. Figure 2E (AsPC-1) and Figure 2F (PANC-1) show that LPA induced ERK1/2 and AKT phosphorylation in both PDAC cells. These results confirmed that LPA activated LPA-LPAR signaling, which resulted in the activation of the migratory activity of PDAC cells.

3.3 | LPC promoted LPA-LPAR signaling via the phosphorylation of ERK1/2 and AKT, which was regulated by ATX

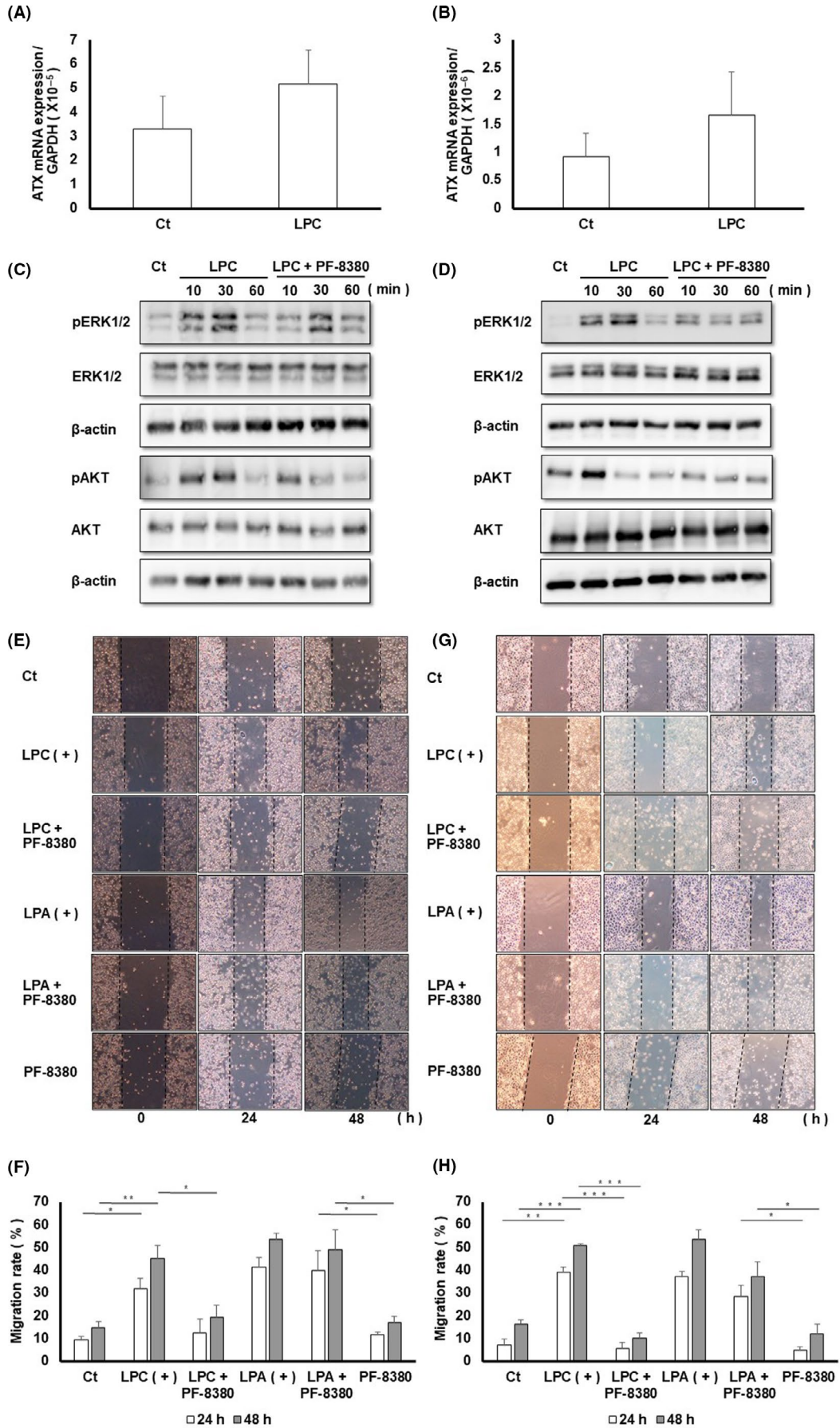
Lysophosphatidylcholine is an LPA precursor that is hydrolyzed to LPA by ATX activity. As shown in Figure 3A,B, we confirmed that a significant amount of ATX was being stably expressed in PDAC cells, and the expression was slightly upregulated by LPC administration.

We also checked the phosphorylation of ERK1/2 and AKT to investigate the biological status of the signaling activated by the LPA precursor. LPC also induced ERK1/2 and AKT phosphorylation as well as LPA. However, treatment with an ATX inhibitor, PF-8380, suppressed the LPC-induced ERK1/2 and AKT phosphorylation (Figure 3C,D). These results confirmed that LPC, as well as LPA, activated the MAPK pathway and PI3K pathway, and its biological activity was ATX-dependent.

3.4 | ATX inhibition suppressed the migration and proliferation of PDAC cells

Next, we conducted the wound-healing assay to evaluate the effects of ATX on PDAC cell migration. Compared with the control,

FIGURE 3 Autotaxin (ATX) mRNA, protein expression, and cell migration in AsPC-1 and PANC-1 cells. RT-PCR analysis of ATX in AsPC-1 (A) and PANC-1 (B) cells. One hour after the addition of 0.1% BSA (Ct) or 10 $\mu\text{mol/L}$ lysophosphatidylcholine (LPC), we harvested mRNA. Data represent the means of three independent experiments. Bars, standard error. Western blotting analysis of ERK1/2 and AKT phosphorylation after the addition of 10 $\mu\text{mol/L}$ LPC plus 0.1% BSA or 10 $\mu\text{mol/L}$ LPC plus 10 $\mu\text{mol/L}$ PF-8380 in AsPC-1 (C) and PANC-1 (D) cells. Representative images obtained at 0, 24, and 48 h after a scratch wound was made in confluent monolayers of AsPC-1 (E) and PANC-1 (G) cells. At 0 and 24 h after the scratch, 0.1% BSA (Ct), 10 $\mu\text{mol/L}$ LPC only (LPC [+]), 10 $\mu\text{mol/L}$ LPC plus 10 $\mu\text{mol/L}$ PF-8380 (LPC + PF-8380), 10 $\mu\text{mol/L}$ LPA only (LPA [+]), 10 $\mu\text{mol/L}$ LPA plus 10 $\mu\text{mol/L}$ PF-8380 (LPA + PF-8380), or 10 $\mu\text{mol/L}$ PF-8380 only (PF-8380) was added. In addition, 0.1% BSA was added as a control. Quantification of the wound-healing assay in AsPC-1 (F) and PANC-1 (H) cells. Data represent the means of three independent experiments. Bars, standard error; * $P < .05$; ** $P < .01$; *** $P < .001$



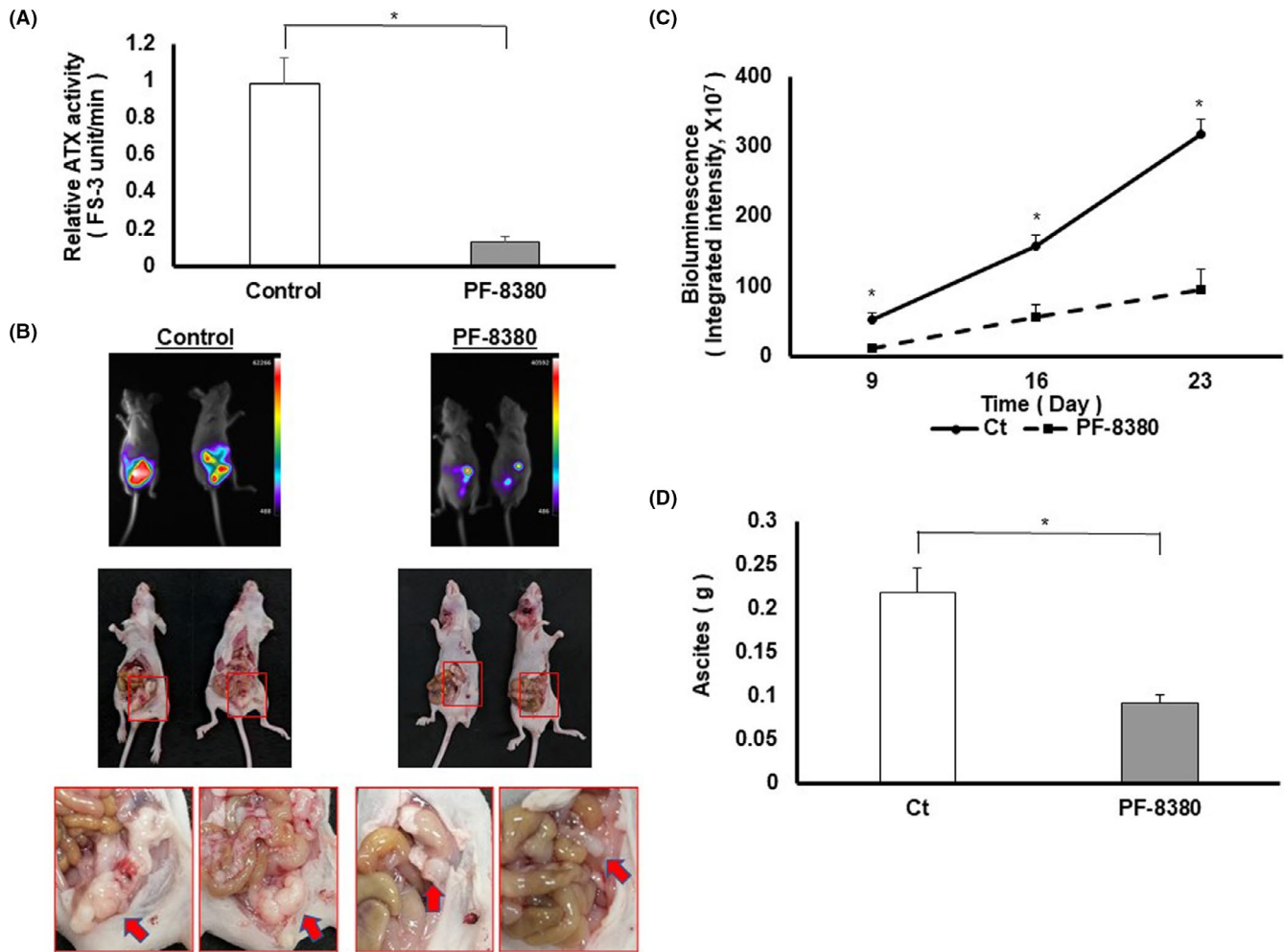


FIGURE 4 Assessment of peritoneal dissemination in an in vivo peritoneal dissemination model. A, Measurement of autotaxin (ATX) activity in murine serum. PF-8380, solubilized in 2:1 dimethyl sulfoxide (DMSO)-saline, was injected intraperitoneally at the dose of 10 mg/kg body weight twice a day for 3 d. Using the ATX Activity Kit, ATX activity in the serum collected 8 h after the last PF-8380 injection or DMSO-saline injection in the control group was measured. Data represent the means of the control group ($n = 8$) or PF-8380 group ($n = 3$). Bars, standard error; * $P < .01$. B, Representative images of nude mice with peritoneal dissemination on day 23 after AsPC1/luc cell implantation. Upper, bioluminescence imaging; middle, image under white light; lower, magnified images of peritoneal disseminated tumors. Red arrows indicate the peritoneal disseminated tumors. C, Quantification of bioluminescence imaging. Data represent the means of the control group ($n = 11$) and the PF-8380 group ($n = 13$). Bars, standard error; * $P < .001$. D, Measurement of the amount of ascites. Data represent the means of the control group ($n = 11$) and PF-8380 group ($n = 13$). Bars, standard error; * $P < .001$

LPC significantly promoted the migration in both AsPC-1 (48 hours, $15\% \pm 2.8\%$ vs $45\% \pm 5.6\%$, $P < .01$) and PANC-1 (48 hours, $16\% \pm 1.6\%$ vs $51\% \pm 0.8\%$, $P < .001$) cells as well as LPA. In contrast, PF-8380 treatment significantly suppressed the migration induced by LPC in both AsPC-1 (48 hours, $45\% \pm 5.6\%$ vs $19\% \pm 5.4\%$, $P < .05$) and PANC-1 (48 hours, $51\% \pm 0.8\%$ vs $10\% \pm 2.1\%$, $P < .001$) cells, although PF-8380 alone did not influence the migratory activity of PDAC cells, and PF-8380 treatment did not suppress the LPA-induced migration in both PDAC cells (Figure 3E-H). In addition, PF-8380 treatment significantly suppressed cell proliferation induced by LPC in both AsPC-1 (cell number; 48 hours, $19.7 \times 10^4 \pm 0.4 \times 10^4$ vs $15.6 \times 10^4 \pm 0.5 \times 10^4$, $P < .001$) and

PANC-1 (48 hours, $21.6 \times 10^4 \pm 1.0 \times 10^4$ vs $11.6 \times 10^4 \pm 0.4 \times 10^4$, $P < .001$) cells. However, PF-8380 alone did not influence the proliferate activity of PDAC cells (Figure S3C,D). These results suggested that the ATX inhibitor suppressed the migratory and proliferate activity of PDAC cells via the modulation of LPC-derived LPA signaling.

Furthermore, we verified the effects of ATX on PDAC cell migration with RNA interference knockdown cells. As expected, ATX knockdown significantly suppressed the migration induced by LPC in both AsPC-1 (48 hours, $41.8\% \pm 1.7\%$ vs $11.9\% \pm 1.0\%$, $P < .001$) and PANC-1 (48 hours, $35.7\% \pm 3.9\%$ vs $10.9\% \pm 3.0\%$, $P < .05$) cells (Figure S4A-F). These results were consistent with the results of the ATX inhibitor.

3.5 | ATX inhibitor suppressed PDAC progression in a murine peritoneal dissemination model

Prior to the *in vivo* study, we intraperitoneally injected 10 mg/kg PF-8380 dissolved in DMSO (25 mg PF-8380 plus 8.3 mL DMSO) twice a day in nude mice for 3 days and then measured the ATX activity in the sera of the nude mice (control group, $n = 8$; PF-8380 group, $n = 3$). We confirmed that this protocol could provide satisfactory pharmacological effects for inhibiting ATX activity (suppression rate of 86.5%, $P < .01$; Figure 4A). To investigate the roles and effects of ATX on peritoneal dissemination and malignant ascites, 10 mg/kg PF-8380 was intraperitoneally injected into nude mice with intraperitoneally implanted AsPC1/luc cells. There was no significant body weight loss in the control and treatment groups during the treatment (data not shown), which suggested that the volume of PF-8380 used was not harmful to the mice. During the treatment protocol, we monitored the states of intraperitoneal dissemination with bioluminescence imaging. Mice without any fluorescent signals under IVIS at 1 week after implantation were excluded, and finally, 11 mice in the control group and 13 mice in the treatment group were included in this experiment. We could detect the strong inhibitory effect of PF-8380 on intraperitoneal dissemination as it was

clearly visualized by bioluminescence imaging and under white-light imaging (Figure 4B). Quantified data from bioluminescence imaging proved that PF-8380 significantly reduced the total volume of intraperitoneal dissemination compared with the control group (bioluminescence, integrated intensity; day 23, $317.4 \times 10^7 \pm 21.6 \times 10^7$ vs $94.4 \times 10^7 \pm 30.3 \times 10^7$, $P < .001$; Figure 4C). We also observed that PF-8380 significantly decreased the amount of ascites compared with the control group (0.22 ± 0.03 g vs 0.09 ± 0.01 g, $P < .001$; Figure 4D). These results suggested that ATX inhibition could suppress intraperitoneal dissemination and reduce ascites in PDAC.

Using tumor samples, Western blotting analysis was performed for biological investigation. Compared with the control group, the treatment group had lower expression levels of proliferating cell nuclear antigen (PCNA), which is a marker of proliferation. In terms of the expression of cleaved caspase-3, which is a marker of an apoptosis, some samples from the treatment group showed evident expression of cleaved caspase-3, while others did not; in contrast, no detectable expression was observed in the control group (Figure 5A). In the immunohistochemical analysis, the number of Ki67-positive cells was significantly suppressed in the PF-8380 treatment group ($43.9\% \pm 2.1\%$ vs $24.6\% \pm 6.1\%$, $P < .01$; Figure 5B,C) compared with the control group, although the expression level of cleaved

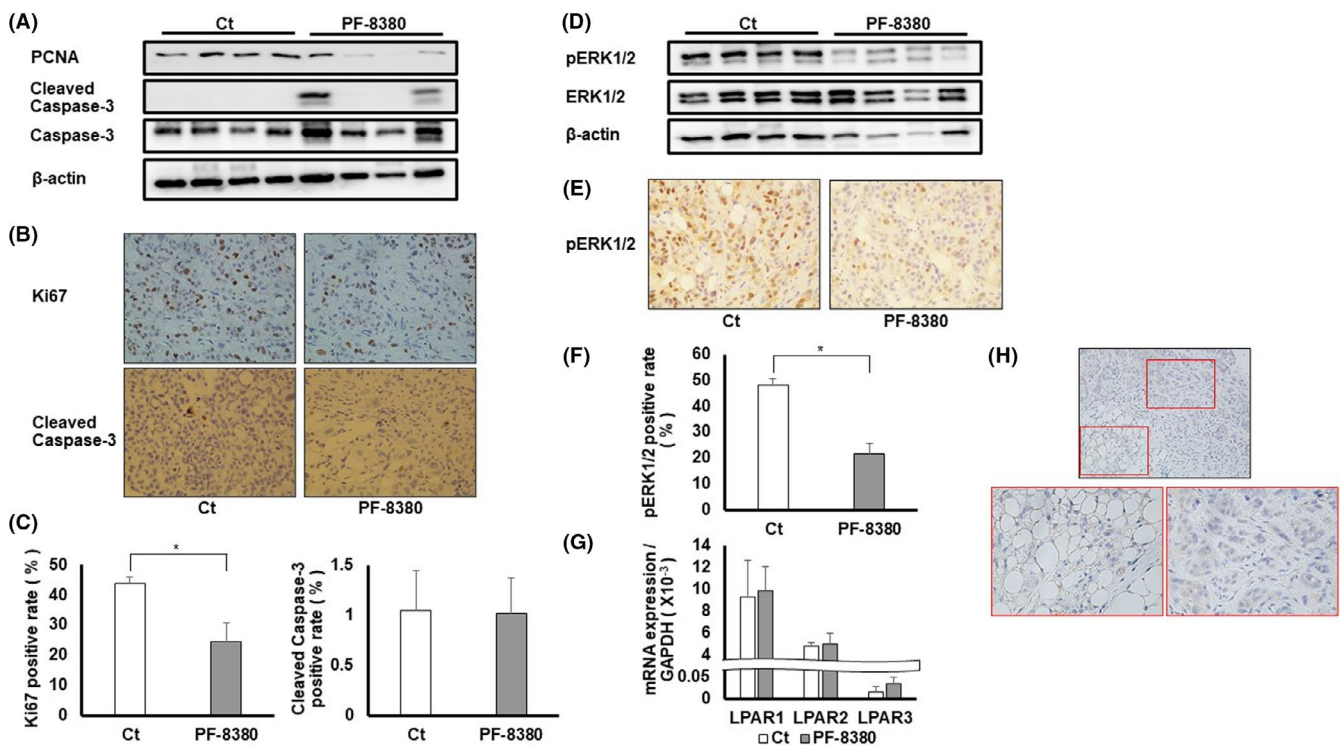


FIGURE 5 Western blot, immunohistochemical, and RT-PCR analysis of disseminated peritoneal tumors. A, Representative Western blotting analysis of PCNA and cleaved caspase-3 in the two groups. B, Representative immunohistochemical images of Ki67 and cleaved caspase-3 in the two groups. C, Quantification of Ki67 and cleaved caspase-3-positive cells in the two groups. Data represent the means of the control group ($n = 11$) and PF-8380 group ($n = 9$). Bars, standard error; $*P < .01$. D, Representative Western blotting analysis of ERK1/2 phosphorylation in the two groups. E, Representative immunohistochemical images of ERK1/2 phosphorylation in the two groups. F, Quantification of phospho-ERK1/2-positive cells in the two groups. Data represent the means of the control group ($n = 11$) and PF-8380 group ($n = 9$). Bars, standard error; $*P < .001$. G, RT-PCR analysis of LPAR1-3 in the two groups. Data represent the means of the control group ($n = 3$) and PF-8380 group ($n = 3$). Bars, standard error. H, Representative immunohistochemical images of autotaxin (ATX) in the peritoneal dissemination model. Insets show magnified views of the boxed area. Left box, adipose tissues; right box, cancer cells

caspace-3 did not differ significantly in either group ($1.0\% \pm 0.4\%$ vs $1.0\% \pm 0.3\%$; Figure 5B,C). In addition, Western blotting analysis revealed that the treatment group had a lower ERK1/2 phosphorylation level (Figure 5D) than the control group; this was consistent with the results of the immunohistochemical analysis ($48.4\% \pm 2.3\%$ vs $21.7\% \pm 4.0\%$, $P < .001$; Figure 5E,F). It was also confirmed that the mRNA expression level of LPAR1-3 in tumors did not differ significantly between the control and treatment groups (Figure 5G), which could validate the consistency of the subsequent circumstance after ATX-LPA signaling. Moreover, we confirmed that ATX staining was observed in both peritoneal disseminated tumors which were originally implanted and adjacent adipose tissues (Figure 5H). These results suggested that the ATX inhibitor suppressed disseminated tumor proliferation via the suppression of LPA production and the subsequent MAPK signaling; this was consistent with the results of the *in vivo* study.

3.6 | The correlation between the degree of peritoneal dissemination and the amount of ATX in ascites

We next focused on the characteristics and correlations among the tumor volume, the amount of ascites, and the amounts of ATX in ascites and serum. Possibly due to experimental error,

data on ATX could not be obtained within the detectable range for two mouse samples from the PF-8380 group, and they were excluded from the analysis. Eleven mice in the control group and 11 mice in the treatment group were finally included in this experiment. Although the amount of ATX in serum did not show any positive correlation with the other factors that indicate the status of cancer progression, there was a significant positive correlation between the amount of ATX in ascites and the integrated tumor volume ($R = .572$, $P < .01$; Figure 6A,C). There was also a significant positive correlation between the integrated volume of peritoneal tumors and the volume of ascites ($R = .552$, $P < .01$; Figure 6B,C). These results revealed that, unlike ATX in serum, there was a positive correlation between the degree of disseminated cancer progression and the amount of ATX in ascites, indicating that ATX in ascites could not only contribute to the promotion of intraperitoneal dissemination but also work as a tumor marker in ascites.

4 | DISCUSSION

Many molecular targeted therapies for PDAC, such as the targeting of growth factor receptors,²⁴ major downstream pathways,²⁵ and angiogenesis,^{24,26} have been reported in the basic research field. However, none of the many molecular targeted therapies that seemed promising

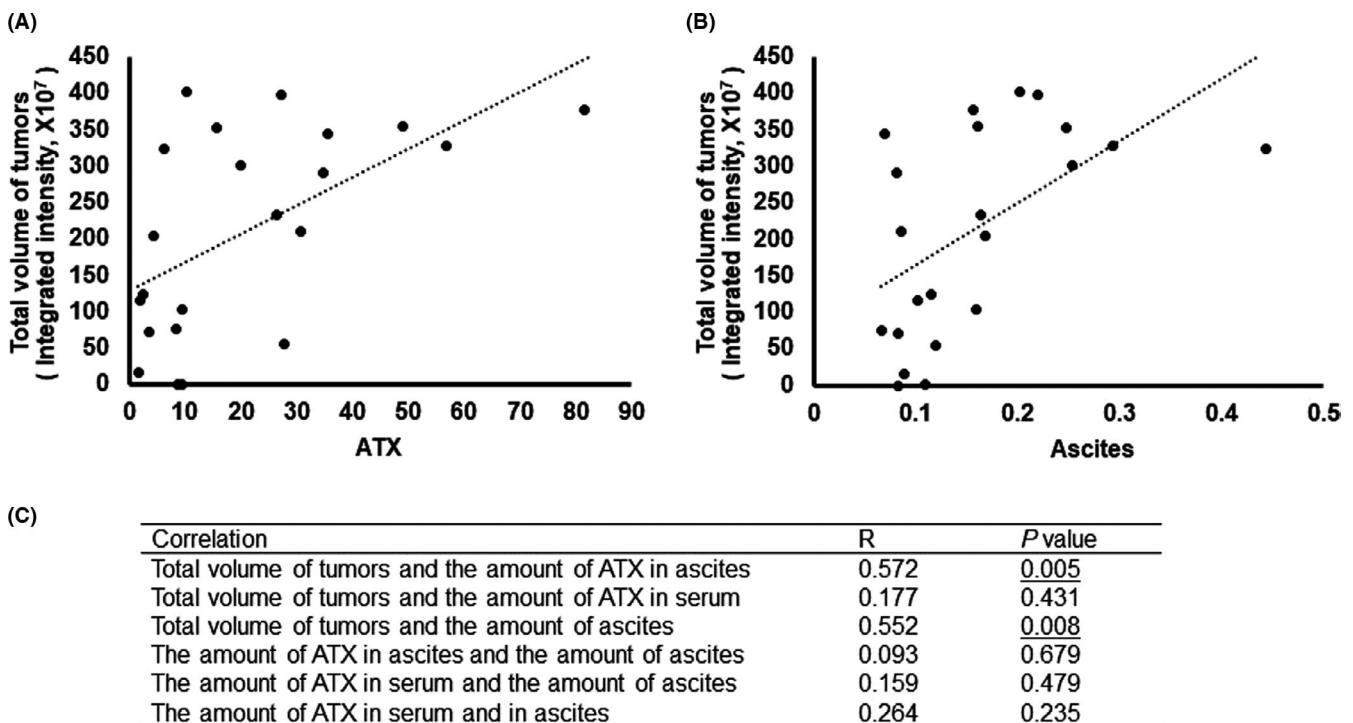


FIGURE 6 Regression analysis of autotaxin (ATX) in murine ascites. A, Data on the correlation between the amount of ATX in ascites and the integrated volume of peritoneal pancreatic ductal adenocarcinoma (PDAC) cells were plotted. B, Data on the correlation between the integrated volume of peritoneal PDAC cells and the amount of ascites were plotted. C, Pearson correlation coefficients among murine liquid samples obtained from the control group ($n = 11$) and PF-8380 group ($n = 11$). R, Pearson correlation coefficient. P-value, statistical analysis for multiple comparisons. Statistically significant correlations are underlined

based on basic research has led to a breakthrough clinical treatment. Moreover, peritoneal dissemination and malignant ascites in PDAC patients are recognized as factors of a poorer outcome.¹⁹

Recent progress in deciphering malignant ascites has unveiled that ascites serve as an important tumor microenvironment that is enriched in protumorigenic signals, which contribute to enhanced invasiveness.^{27,28} In particular, because the PDAC microenvironment suffers from the hypovascular conditions, the presence of ascites has an important role as a special "nutrition source," which must be a notable therapeutic target. We have considerable interest in the ATX-LPA axis in malignant ascites due to the increasing evidence of high levels of LPA in ascites of ovarian cancers²⁹ and high levels of serum ATX in PDAC.¹⁸

The expression of LPA and LPARs is upregulated in various cancers. LPARs transmit and activate downstream signals, such as the MAPK pathway, and LPA signaling modulates cancer progression.^{6,7} To confirm the biological evidence showing that LPA-LPAR signaling works as a cancer promotor, we validated that LPA promoted cell migration via LPA-LPAR signaling in PDAC cells.

A reasonable way to regulate LPA signaling is to block LPARs. Some currently available receptor inhibitors that showed good effectiveness in basic research are: Ki16425,³⁰ which is an LPA1, LPA2, and LPA3 antagonist; AM095³¹ and ONO-7300243,³² which are LPA1 antagonists; and Ki16198,³³ which is an LPA1 and LPA3 antagonist. However, these LPAR inhibitors still have not reached clinical application due to toxicity issues. In addition, these LPAR inhibitors are not sufficient in fully regulating LPA signaling due to the selectivity of inhibitors and the variety of LPAR subtypes.³⁴ Another method of regulating LPA signaling is to block LPA itself. However, LPA is an unstable mediator that has a very short half-life of approximately 3 minutes.³⁵ To generate a significant amount of LPA stably, ATX has an important role as the main producer of LPA. The inhibition of ATX is expected to block LPA generation and stop LPA signaling. We first discovered that ATX expression was remarkably increased in murine ascites compared with murine serum in PDAC.

Various cancers have been reported to secrete ATX, which contributes to their autocrine and paracrine activities. In terms of PDAC, datasets obtained from databases have validated that the copy number of the gene encoding ATX (*enpp2* gene) is elevated in 8% to 11% of PDAC patients (Figure S5); this was corroborated by our *in vitro* data.

To further understand the roles of ATX in PDAC, we clarified that ATX inhibition suppressed cell migration via inhibition of the MAPK pathway and PI3K pathway when LPC was present *in vitro*. Following the *in vitro* results and the novel evidence of increased amounts of ATX in malignant ascites, we successfully demonstrated that the pharmacological inhibition of ATX reduced intraperitoneal dissemination and malignant ascites in an *in vivo* model; this was supported by biological validation showing that the ATX inhibitor suppressed the cell proliferation markers, Ki67 and PCNA, and the MAPK pathway in peritoneal disseminated tumors. Although we could confirm the result of the *in vitro* study showing that the ATX inhibitor suppressed the PI3K pathway, the *in vivo* study could not validate the same result because of the quite wide variability

of immunoblotting and the blurredness of its immunohistochemical staining (data not shown).

Autotaxin is secreted not only by tumor cells but also by cells of the tumor environment,¹⁰ where it prepares a metastatic niche and promotes invasion.^{36,37} Stromal ATX has been highlighted in the bone metastasis of breast carcinoma.³⁸⁻⁴¹ The stromal cellular components of ascites mainly include fibroblasts, endothelial or mesothelial cells, adipose tissue-derived stromal cells, bone marrow-derived stem cells, immune cells, and adipocytes. Adipocytes are important structural components of the peritoneal cavity. Apart from cancer cells, adipocytes are well-known as a rich source of stromal ATX.^{42,43} The results of immunochemical analysis for ATX with peritoneal disseminated tumors and the adjacent tissues are contributory to prove that ATX can be derived from both cancer cells and noncancer cells. Although further studies are needed to clarify the other components that act as ATX producers, the increasing evidence and our present data strongly support the logic that ATX is supplied by both cancer and noncancer cellular components in malignant ascites, and that increased levels of ATX in enriched ascites accelerate PDAC development.

The management of ascites is important for PDAC patients. In the past, studies have attempted to treat ascites by intraperitoneally injecting chemotherapeutic agents because PDAC survives in hypovascular microenvironment.^{44,45} In the present study, we noted that the amount of ATX increased in malignant ascites, and we showed that the pharmacological inhibition of ATX by the intraperitoneal administration of an ATX inhibitor successfully suppressed the burden of ascites. In addition, we found that ATX in malignant ascites was a potential biomarker because there was a positive correlation between the amount of ATX in ascites and the integrated peritoneal dissemination of tumors. These results obtained from *in vitro* and *in vivo* studies would require further clinical validation with clinical samples.

In conclusion, we proved that the intraperitoneal administration of an ATX inhibitor suppressed peritoneal dissemination and malignant ascites in an *in vivo* PDAC peritoneal dissemination model as well as in *in vitro* experiments. This is because ATX was abundant in malignant ascites, and the inhibition of ATX suppressed the ATX-LPA axis and LPA signaling. We strongly believe that (a) ATX is a promising biomarker in malignant ascites, and (b) ATX inhibition will become a new molecular targeted therapy for advanced PDAC, notably for peritoneal dissemination and malignant ascites.











ACKNOWLEDGMENTS

This study was supported by grants from the Japan Society for the Promotion of Science (KAKENHI Grant Numbers KK17K09466 and KK20K08291).

DISCLOSURE

The authors have no conflict of interest.

ORCID

- Naruomi Jinno  <https://orcid.org/0000-0002-2634-2338>
- Michihiro Yoshida  <https://orcid.org/0000-0002-4167-2781>
- Kazuki Hayashi  <https://orcid.org/0000-0001-5217-2873>
- Itaru Naitoh  <https://orcid.org/0000-0001-8342-886X>
- Yasuki Hori  <https://orcid.org/0000-0001-9510-2568>
- Makoto Natsume  <https://orcid.org/0000-0002-1716-0583>
- Akihisa Kato  <https://orcid.org/0000-0002-7733-7854>
- Kenta Kachi  <https://orcid.org/0000-0001-7462-7170>
- Go Asano  <https://orcid.org/0000-0002-1528-7572>
- Naoki Atsuta  <https://orcid.org/0000-0002-3563-0614>
- Hidegori Sahashi  <https://orcid.org/0000-0003-3983-593X>
- Hiroki Kataoka  <https://orcid.org/0000-0001-9491-0723>

REFERENCES

- Zhou Y, Wang K, Zhou Y, et al. HEATR1 deficiency promotes pancreatic cancer proliferation and gemcitabine resistance by up-regulating Nrf2 signaling. *Redox Biol.* 2019;29:101390.
- Conroy T, Desseigne F, Ychou M, et al. FOLFIRINOX versus gemcitabine for metastatic pancreatic cancer. *N Engl J Med.* 2011;364:1817-1825.
- Von Hoff DD, Ervin T, Arena FP, et al. Increased survival in pancreatic cancer with nab-paclitaxel plus gemcitabine. *N Engl J Med.* 2013;369:1691-1703.
- Lin ME, Herr DR, Chun J. Lysophosphatidic acid (LPA) receptors: signaling properties and disease relevance. *Prostaglandins Other Lipid Mediat.* 2010;91:130-138.
- Yun CC, Kumar A. Diverse roles of LPA signaling in the intestinal epithelium. *Exp Cell Res.* 2015;333:201-207.
- Yun CC. Lysophosphatidic acid and autotaxin-associated effects on the initiation and progression of colorectal cancer. *Cancers (Basel).* 2019;11:958.
- Benesch MGK, MacIntyre ITK, McMullen TPW, Brindley DN. Coming of age for autotaxin and lysophosphatidate signaling: clinical applications for preventing, detecting and targeting tumor-promoting inflammation. *Cancers (Basel).* 2018;10:73.
- Fukushima K, Takahashi K, Yamasaki E, et al. Lysophosphatidic acid signaling via LPA1 and LPA3 regulates cellular functions during tumor progression in pancreatic cancer cells. *Exp Cell Res.* 2017;352:139-145.
- Fukushima K, Otagaki S, Takahashi K, et al. Promotion of cell-invasive activity through the induction of LPA receptor-1 in pancreatic cancer cells. *J Recept Signal Transduct Res.* 2018;38:367-371.
- Tigyi GJ, Yue J, Norman DD, et al. Regulation of tumor cell - Microenvironment interaction by the autotaxin-lysophosphatidic acid receptor axis. *Adv Biol Regul.* 2019;71:183-193.
- Stracke ML, Krutzsch HC, Unsworth EJ, et al. Identification, purification, and partial sequence analysis of autotaxin, a novel motility-stimulating protein. *J Biol Chem.* 1992;267:2524-2529.
- Ninou I, Magkrioti C, Aidinis V. Autotaxin in pathophysiology and pulmonary fibrosis. *Front Med (Lausanne).* 2018;5:180.
- Kaffe E, Katsifa A, Xylourgidis N, et al. Hepatocyte autotaxin expression promotes liver fibrosis and cancer. *Hepatology.* 2017;65:1369-1383.
- Benesch MG, Ko YM, Tang X, et al. Autotaxin is an inflammatory mediator and therapeutic target in thyroid cancer. *Endocr Relat Cancer.* 2015;22:593-607.
- Kishi Y, Okudaira S, Tanaka M, et al. Autotaxin is overexpressed in glioblastoma multiforme and contributes to cell motility of glioblastoma by converting lysophosphatidylcholine to lysophosphatidic acid. *J Biol Chem.* 2006;281:17492-17500.
- Yang SY, Lee J, Park CG, et al. Expression of autotaxin (NPP-2) is closely linked to invasiveness of breast cancer cells. *Clin Exp Metastasis.* 2002;19:603-608.
- Yang Y, Mou L, Liu N, Tsao MS. Autotaxin expression in non-small-cell lung cancer. *Am J Respir Cell Mol Biol.* 1999;21:216-222.
- Nakai Y, Ikeda H, Nakamura K, et al. Specific increase in serum autotaxin activity in patients with pancreatic cancer. *Clin Biochem.* 2011;44:576-581.
- Baretti M, Pulluri B, Tsai HL, et al. The significance of ascites in patients with pancreatic ductal adenocarcinoma: a case-control study. *Pancreas.* 2019;48:585-589.
- Takahara N, Isayama H, Nakai Y, et al. Pancreatic cancer with malignant ascites: clinical features and outcomes. *Pancreas.* 2015;44:380-385.
- Kato A, Kataoka H, Yano S, et al. Maltotriose conjugation to a chlorin derivative enhances the antitumor effects of photodynamic therapy in peritoneal dissemination of pancreatic cancer. *Mol Cancer Ther.* 2017;16:1124-1132.
- Reinartz S, Lieber S, Pesek J, et al. Cell type-selective pathways and clinical associations of lysophosphatidic acid biosynthesis and signaling in the ovarian cancer microenvironment. *Mol Oncol.* 2019;13:185-201.
- Yamada T, Sato K, Komachi M, et al. Lysophosphatidic acid (LPA) in malignant ascites stimulates motility of human pancreatic cancer cells through LPA1. *J Biol Chem.* 2004;279:6595-6605.
- Borja-Cacho D, Jensen EH, Saluja AK, Buchsbaum DJ, Vickers SM. Molecular targeted therapies for pancreatic cancer. *Am J Surg.* 2008;196:430-441.
- Van Cutsem E, van de Velde H, Karasek P, et al. Phase III trial of gemcitabine plus tipifarnib compared with gemcitabine plus placebo in advanced pancreatic cancer. *J Clin Oncol.* 2004;22:1430-1438.
- Adamska A, Domenichini A, Falasca M. Pancreatic ductal adenocarcinoma: current and evolving therapies. *Int J Mol Sci.* 2017;18(7):1338.
- Kim S, Kim B, Song YS. Ascites modulates cancer cell behavior, contributing to tumor heterogeneity in ovarian cancer. *Cancer Sci.* 2016;107:1173-1178.
- Kim S, Gwak H, Kim HS, Kim B, Dhanasekaran DN, Song YS. Malignant ascites enhances migratory and invasive properties of ovarian cancer cells with membrane bound IL-6R in vitro. *Oncotarget.* 2016;7:83148-83159.
- Onallah H, Davidson B, Reich R. Diverse effects of lysophosphatidic acid receptors on ovarian cancer signaling pathways. *J Oncol.* 2019;2019:7547469.
- David M, Ribeiro J, Descotes F, et al. Targeting lysophosphatidic acid receptor type 1 with Debio 0719 inhibits spontaneous metastasis dissemination of breast cancer cells independently of cell proliferation and angiogenesis. *Int J Oncol.* 2012;40:1133-1141.
- Park SJ, Lee KP, Im DS. Action and signaling of lysophosphatidylethanolamine in MDA-MB-231 breast cancer cells. *Biomol Ther.* 2014;22:129-135.
- Terakado M, Suzuki H, Hashimura K, et al. Discovery of ONO-7300243 from a novel class of lysophosphatidic acid receptor 1 antagonists: from hit to lead. *ACS Med Chem Lett.* 2016;7:913-918.
- Komachi M, Sato K, Tobo M, et al. Orally active lysophosphatidic acid receptor antagonist attenuates pancreatic cancer invasion and metastasis in vivo. *Cancer Sci.* 2012;103:1099-1104.
- Yung YC, Stoddard NC, Chun J. LPA receptor signaling: pharmacology, physiology, and pathophysiology. *J Lipid Res.* 2014;55:1192-1214.
- Albers HM, Dong A, van Meeteren LA, et al. Boronic acid-based inhibitor of autotaxin reveals rapid turnover of LPA in the circulation. *Proc Natl Acad Sci USA.* 2010;107:7257-7262.

36. Gotoh M, Fujiwara Y, Yue J, et al. Controlling cancer through the autotaxin-lysophosphatidic acid receptor axis. *Biochem Soc Transac.* 2012;40:31-36.
37. Lee SC, Fujiwara Y, Liu J, et al. Autotaxin and LPA1 and LPA5 receptors exert disparate functions in tumor cells versus the host tissue microenvironment in melanoma invasion and metastasis. *Mol Cancer Res.* 2015;13:174-185.
38. Boucharaba A, Serre CM, Grès S, et al. Platelet-derived lysophosphatidic acid supports the progression of osteolytic bone metastases in breast cancer. *J Clin Investig.* 2004;114:1714-1725.
39. Boucharaba A, Serre CM, Guglielmi J, Bordet JC, Clézardin P, Peyruchaud O. The type 1 lysophosphatidic acid receptor is a target for therapy in bone metastases. *Proc Natl Acad Sci USA.* 2006;103:9643-9648.
40. Leblanc R, Houssin A, Peyruchaud O. Platelets, autotaxin and lysophosphatidic acid signalling: win-win factors for cancer metastasis. *Br J Pharmacol.* 2018;175:3100-3110.
41. Leblanc R, Lee SC, David M, et al. Interaction of platelet-derived autotaxin with tumor integrin $\alpha V\beta 3$ controls metastasis of breast cancer cells to bone. *Blood.* 2014;124:3141-3150.
42. van Meeteren LA, Ruurs P, Stortelers C, et al. Autotaxin, a secreted lysophospholipase D, is essential for blood vessel formation during development. *Mol Cell Biol.* 2006;26:5015-5022.
43. Ferry G, Tellier E, Try A, et al. Autotaxin is released from adipocytes, catalyzes lysophosphatidic acid synthesis, and activates preadipocyte proliferation. Up-regulated expression with adipocyte differentiation and obesity. *J Biol Chem.* 2003;278:18162-18169.
44. Kuwahara K, Sasaki T, Kobayashi K, et al. Gemcitabine suppresses malignant ascites of human pancreatic cancer: correlation with VEGF expression in ascites. *Oncol Rep.* 2004;11:73-80.
45. Uzunparmak B, Sahin IH. Pancreatic cancer microenvironment: a current dilemma. *Clin Transl Med.* 2019;8:2.

SUPPORTING INFORMATION

Additional supporting information may be found online in the Supporting Information section.

How to cite this article: Jinno N, Yoshida M, Hayashi K, et al. Autotaxin in ascites promotes peritoneal dissemination in pancreatic cancer. *Cancer Sci.* 2021;112:668-678. <https://doi.org/10.1111/cas.14689>